Electronic Supplementary Information

Continuous-feed nanocasting process for the synthesis of bismuth nanowire composites

1 Materials

Pluronics P123 ($EO_{20}PO_{70}EO_{20}$, Mw = 5800), 98% reagent grade tetraethylorthosilicate (TEOS), 65w% nitric acid, 36w% hydrochloric acid, 98.5 % xylenes and 99% n-butanol were purchased from Sigma Aldrich. 99.999% bismuth(III) oxide and 98% hydrazine monohydrate were supplied by Alfa Aesar. 99% toluene and 98% methanol were supplied by Fiers, while 97% n-octane was purchased from TCI Europe N.V. All reagents were used as received.

2 Characterization

X-Ray powder Diffraction (XRD) patterns were recorded on a Thermo Scientific ARL X'TRA X-Ray Diffractometer with the Bragg–Brentano theta-2 theta configuration and using Cu Ka radiation. Topas Academic V4.1 software was used for Rietveld refinement[1]. Nitrogen sorption experiments were performed at 77 K with a Micromeritics TriStar 3000 device. Samples were vacuum dried at 120 °C for 12 h prior to analysis. The surface area was calculated using the BET method while the pore-size distribution was determined by analysis of the adsorption branch of the isotherms using the BJH method. Thermogravimetric analysis (TGA) was performed on a NETZSCH STA 449-F3 Jupiter device and TEM images were taken with a JEOL JSM-207 7600F device. X-ray fluorescence (XRF) measurements were performed on a Rigaku NEXCG device under helium atmosphere and RX5 target.

3 SBA-15 and KIT-6 mesoporous silica templates

SBA-15 was synthesized by dissolving 4 g P123 in 120 mL 2 mol/L HCl solution and 30 mL distilled water at RT. Next, the solution was heated to 45 °C and 9.1 mL TEOS was added while vigorously stirring for 5 h. Subsequently, the mixture was aged at 90 °C for 18 h under static conditions. Finally, the precipitate was collected via filtration, dried overnight at RT, and calcinated at 550 °C for 6 h in air with a heating rate of 2 °C/min.[2]

KIT-6 was synthesized by dissolving 4 g P123 in 150 mL 0.5 mol/L HCl solution and 4.9 mL butanol at RT. Next the solution was heated to 35 °C and 9.2 mL TEOS was added while vigorous stirring. The mixture was stirred at that temperature for 24 h and subsequently aged at 90 °C for 24 h under static conditions. Finally, the precipitate was collected via filtration, dried overnight at RT and calcinated at 550 °C for 6 h in air with a heating rate of 2 °C/min.[3] Low angle X-ray powder diffraction data (XRPD) of SBA-15 and KIT-6 are shown in Figure ESI 1a, indicating that the synthesized KIT-6 mesoporous silica possesses a cubic, interconnected pore system with the $Ia\bar{3}d$-space group symmetry, while SBA-15 shows a $P6mm$ hexagonal ordered pore system. Figure ESI 1b and c show respectively the N_2 sorption

isotherms and the BJH pore size distribution plot of both silica templates. The pore diameter according to the BJH model was calculated on the desorption branch of the isotherm. Typically, SBA-15 had pores with a diameter of approximately 7.5 nm. The BET surface area and pore volume were typically between 600 and 1000 m^2/g and 0.7 to 1 mL/g, respectively. The pore diameter of KIT-6 was generally approximately 7 nm, while the BET surface area ranged from 700 to 900 m^2/g and the pore volume from 0.8 to 1.2 mL/g. SBA-15 was used as template material for the synthesis of Bi nanowires for TEM analysis, while KIT-6 mesoporous silica was used as template for the preparation of mesoporous Bi for N_2 sorption analysis and for the electric measurements of a Bi – SiO_2 (KIT-6) nanowire composite.

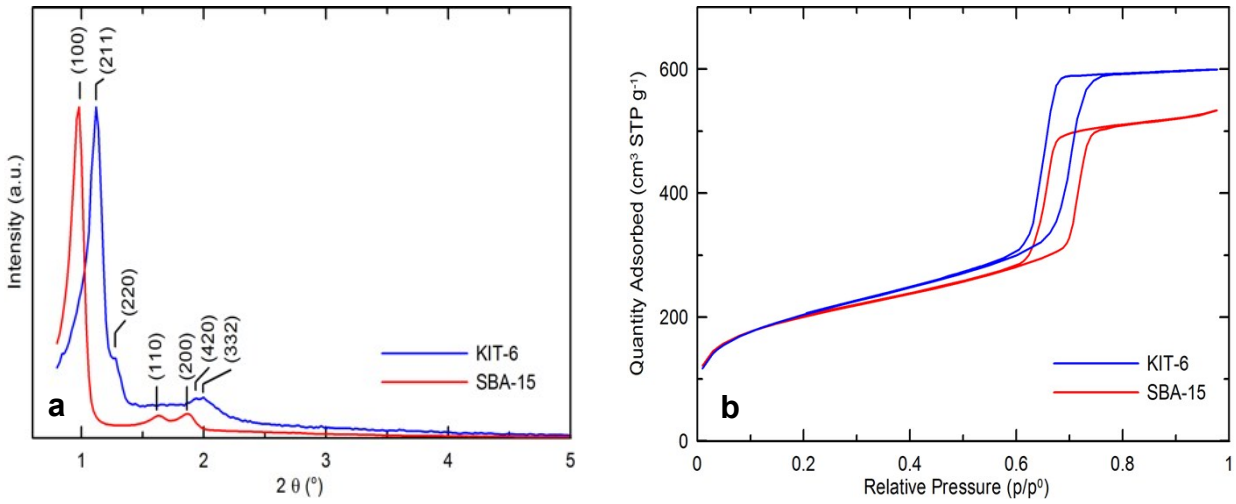

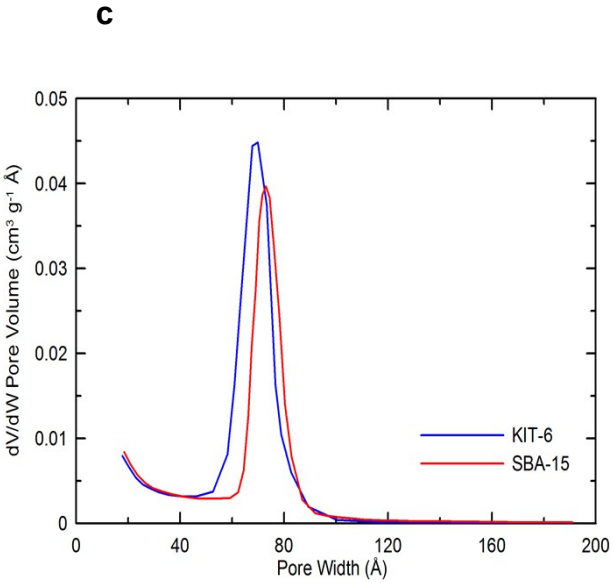

Figure ESI 1. (a) Low angle XRD diffractogram, (b) N_2 sorption isotherms and (c) BJH pore size distribution plot of SBA-15 and KIT-6 mesoporous silica.

4 Continuous-feed nanocasting process

Upon replicating the pore structures of SBA-15 and KIT-6 mesoporous silica, nanowire-like

structures and 3D interconnected "nanowire" networks, respectively, were obtained. A schematic representation of the nanocasting process is shown in Figure ESI 2.

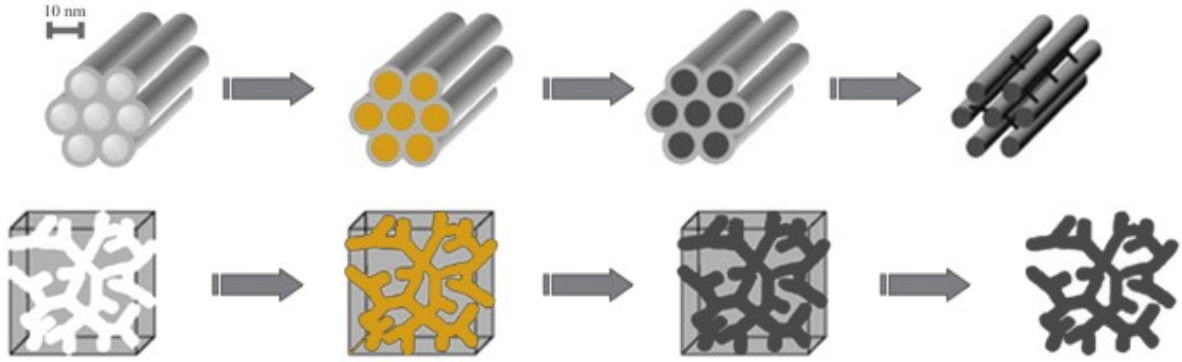

Figure ESI 2. Schematic representation of nanocasting process for (top) SBA-15 and (bottom) KIT-6 mesoporous silica. First, a bismuth precursor solution is impregnated, resulting in the deposition of $BiCl_3$ salt inside the pores. Second, the $BiCl_3$-SiO_2 nanocomposite powder is reduced to Bi – SiO_2. Finally, the nanocomposite powder is either sintered, forming a bulk nanowire composite sample, or the silica is chemically etched, allowing TEM imaging or analysis of the mesoporosity.

The impregnation procedure developed in this research is based on the double solvent method[4] and incipient wetness technique[5]. The example in Figure ESI 3 explains both methods. In Figure ESI 3a-c, a 0.5 mL titania peroxo solution was added to 50 mL toluene. Due to the immiscibility of both solvents, a two-phase system forms. Upon the addition of 1 g SBA-15 with a pore volume of 1 cm^3/g, the coloured solution infiltrates the silica template. Since the volume of precursor solution is lower than the total pore volume of the mesoporous silica, all precursor was impregnated inside the template through capillary impregnation. The term "incipient wetness" indicates that the amount of precursor solution added to the template was less or equal to its pore volume. Consequently, deposition of precursor outside the template is prevented. It can be understood from the example that the template's pores are filled with a diluted precursor solution. Consequently, the amount of metal salt deposited inside the pores depends on the metal concentration of the precursor solution.

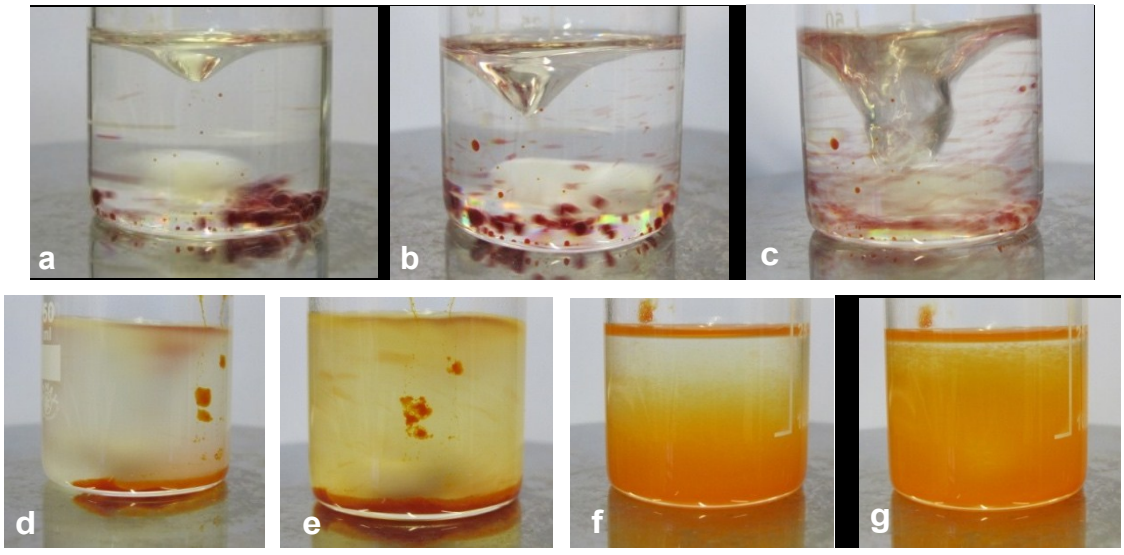

Figure ESI 3. Visual representation of "double solvents" impregnation method: (a-c) a titanium peroxo complex in diluted hydrochloric acid (dark orange aqueous precursor solution) in toluene while vigorously stirring. (d-g) Titania precursor solution in a dispersion of mesoporous silica in toluene after 0, 2, 5, and 10 min stirring, respectively.

In contrast to the double solvent method, the process presented here makes use of refluxing non-polar solvent with a boiling point higher than water, such as toluene, xylene, or n-octane. The polar precursor solution is added continuously and the total volume added is many times larger than the template's pore volume. By means of a Dean-Stark separator, all water from the metal precursor solution is removed from the system while the metal solution immobilizes inside the template's pores, which enables the complete filling of the template with the metal salt by impregnation of a diluted precursor solution. A PFA round bottom flask was used since its hydrophobic properties prevent the wetting of the internal surface or the reaction vessel. The low addition rate of the aqueous precursor solution to the dispersed silica was chosen to ensure that the amount of precursor solution added was always lower than the total pore volume of the template.

Both mesoporous silica templates, SBA-15 and KIT-6, were impregnated using the same procedure described below. Prior to the impregnation of either of the silica templates, the pore volume was measured by means of N_2 sorption analysis to derive the mount of metal salt the pores can contain. The polar precursor solution is defined as an aqueous solution of the precursor salts $BiCl_3$ or $Bi(NO_3)_3.5H_2O$ dissolved in a mixture of precursor solvents, HCl, H_2O, methanol (MeOH) and/or formic acid. The non-polar solvents toluene, xylene, or n-octane are used in such combination that they are immiscible with the polar precursor solution. The different impregnations performed in this study are listed in Table ESI 1.

Table ESI 1. List of impregnation conditions.

Precursor salt	**Precursor solvent**	**Non-polar solvent**	**Precursor addition speed (mL/h)**	**Temperature heater (°C)**
$Bi(NO_3)_3{\cdot}5H_2O$	Water, HNO_3	toluene, xylene, n-octane	4	140-145
$BiCl_3$	Water, HCl, formic acid (FA), methanol	n-octane	4	160-165

The impregnation setup depicted in Figure ESI 4 was used for the synthesis of bismuth nanowires and nanocomposite structures. An aluminium heat exchanger was used for efficient heating of the PFA round bottom flask. A syringe pump was used to inject the precursor solution in a controlled manner, whereas the temperature of the heater controlled the evaporation rate of the aqueous solution. Note that the simplicity of the system did not allow us to monitor the rate of water removal by means of the Dean-Stark separator.

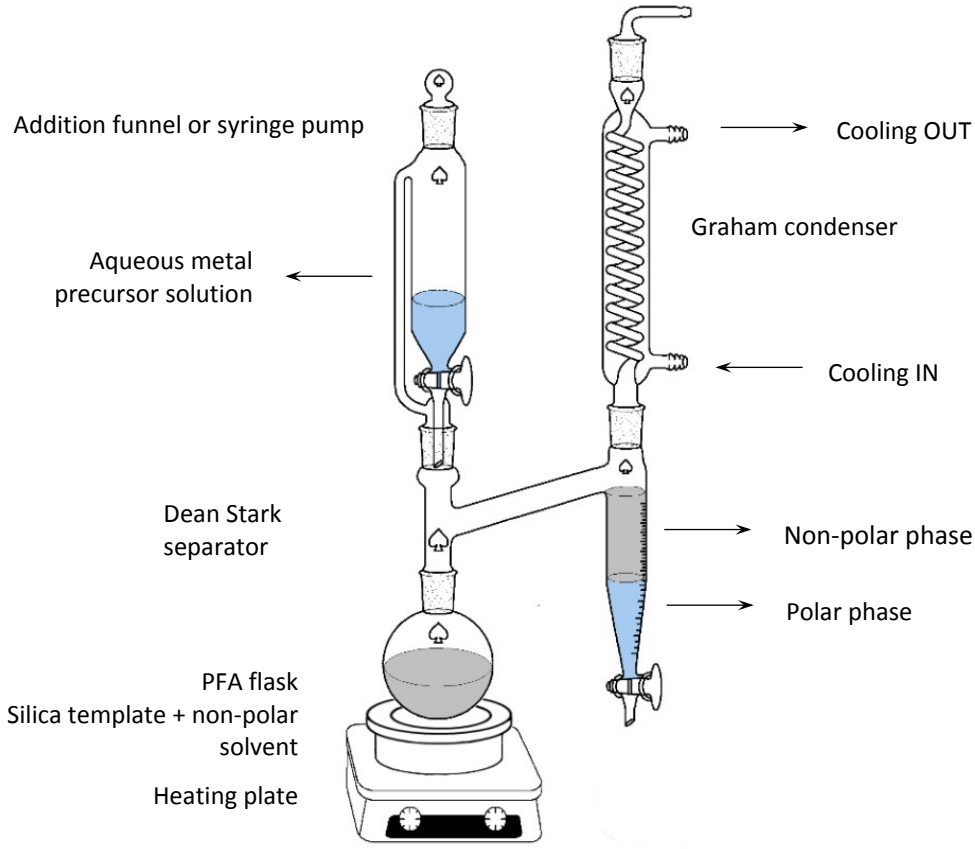

Figure ESI 4. Schematic representation of the continuous-feed nanocasting setup for the impregnation of a polar precursor solution into a mesoporous silica template dispersed in a high-boiling, non-polar solvent. The polar precursor solution is added to the PFA reaction flask at a constant rate and migrates into the pores. Meanwhile, the polar precursor solvent is removed selectively from the system by means of the Dean-Stark separator. The precursor salt or its decomposition product is deposited inside the template's pores. The refluxing solvents boil off and condense in the Graham condenser. Due to the higher density and the immiscibility of both solvents, the aqueous phase is selectively collected in the right arm of the Dean Stark, while the non-polar solvent returns to the system.

Since the bismuth precursor salt $BiCl_3$ hydrolyses in water, an acidified aqueous precursor was prepared. However, we observed from Figure ESI 5 that the metal salt decomposed to BiOCl during the impregnation of a 30 w% HCl and 60 mL methanol, both with and without the addition of 15 mL formic acid in n-octane (bp. 125 °C) as non-polar solvent.

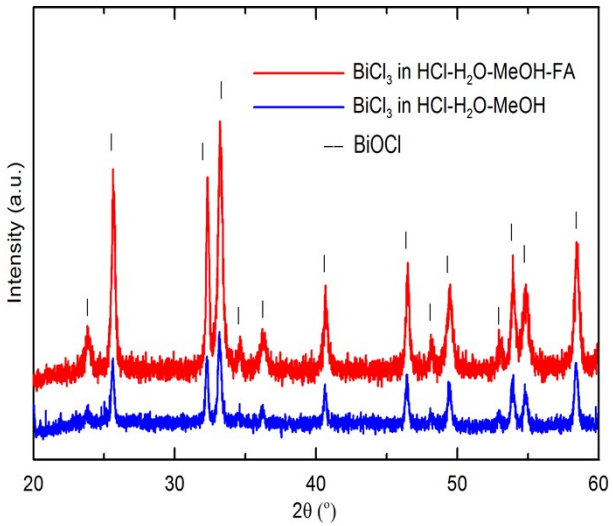

Figure ESI 5. X-ray powder diffraction pattern of SBA-15 mesoporous silica powder impregnated with $BiCl_3$ dissolved in 15 mL 30 w% HCl and 60 mL methanol, with or without 15 mL formic acid (FA), while octane was used as non-polar solvent. It can be seen that the metal salt decomposed to BiOCl as the solvent was removed during the impregnation process.

Since the molecular weight of the precursor salt is typically higher and the density lower than the desired product, volume constriction of the impregnated precursor during the conversion of, e.g., a metal salt to its oxide or metallic form is inevitable. However, the loading efficiency of a certain material can be enhanced if the difference in molecular weight between the decomposed precursor and the target product is reduced. The decomposition of $BiCl_3$ to BiOCl during the impregnation is an example how the pore loading can be enhanced. Table ESI 2 shows the theoretical maximum pore loading efficiencies of $Bi(NO_3)_3.5H_2O$ and $BiCl_3$ depending on their decomposed precursor when they are converted to their metallic form.

Table ESI 2. Theoretical maximum pore loading efficiencies with metallic bismuth depending on the precursor salt used and its decomposition product during the impregnation.

Precursor salt	Decomposed precursor	Target product	Pore loading efficiency (%)
$Bi(NO_3)_3{\cdot}5H_2O$	None ($Bi(NO_3)_3.5H_2O$)	Bi	12.5
$Bi(NO_3)_3{\cdot}5H_2O$	$BiONO_3$	Bi	36.7
$BiCl_3$	None ($BiCl_3$)	Bi	32.2
$BiCl_3$	BiOCl	Bi	60.5

To obtain a better understanding of the decomposition process of the precursor salt during the impregnation, TGA measurements were performed. The thermal decomposition of $Bi(NO_3)_3.5H_2O$ and $BiCl_3$ in air is shown in Figure ESI 6. It can be calculated from the analysed mass loss that the nitrate salt lost 4.4 hydrate water molecules when heated to 108 °C, the boiling temperature of toluene, while a mass loss equivalent to 6 water molecules was obtained at 125 °C, the boiling temperature of n-octane. The latter suggests that on top of the removal of all water molecules of $Bi(NO_3)_3.5H_2O$, the nitrates also

started to decompose. Dry $BiCl_3$, on the other hand, started to decompose only above 250 °C, while a melt was formed at approximately 228 °C (endothermic peak in DTA signal). We believe the drastic weight loss of $BiCl_3$ between approximately 200 and 330 °C was due to sublimation of the salt, which could be suppressed by using humidified air. The decomposition of the precursor salt during impregnation is possible due to the high temperature used during the impregnation, namely, refluxing toluene, n-octane, or xylene. Due to removal of the acidic precursor solvent during the impregnation, the $BiCl_3$ metal salt hydrolysed to BiOCl, while $Bi(NO_3)_3.5H_2O$ decomposed through the loss of hydrate waters. The extent of these effects depends on the boiling temperature of the non-polar solvent.

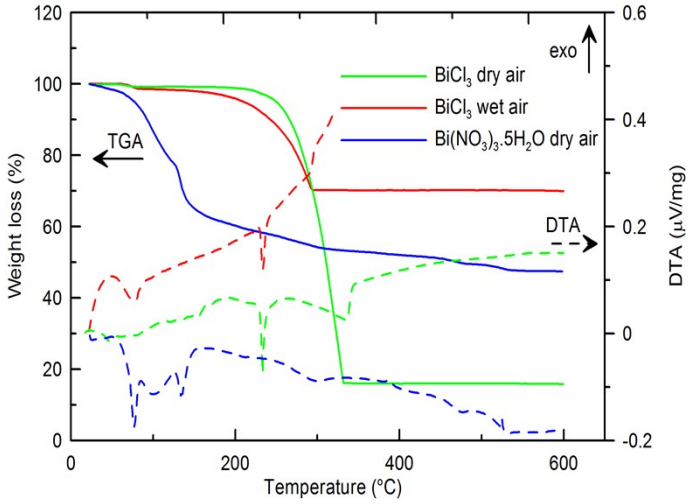

Figure ESI 6. Thermogravimetric analysis of $Bi(NO_3)_3.5H_2O$ and $BiCl_3$ in humidified and dry air at 2 °C/min heating rate. The weight loss due to the loss of hydrate waters is clear from the TGA signal of $Bi(NO_3)_3.5H_2O$. The TGA signal of $BiCl_3$ shows a drastic weight loss in dry air, whereas the weight loss was suppressed in humidified air. The endothermic peak on the DTA signal of $BiCl_3$ shows the formation of a melt at 228 °C.

5 *Reduction of $BiCl_3 – SiO_2$ nano composite powder*

A sealable tube flow furnace (Figure ESI 7) was used for the reduction of $BiCl_3/Bi(NO_3)_3$ – silica composite powder. Approximately 0.5 g of sample was placed in a ceramic crucible and placed in the centre of the furnace. Different reducing agents were tested to reduce $Bi(NO_3)_3.5H_2O$ and $BiCl_3$ to metallic bismuth. However, the low melting point of metallic Bi, 271 °C, was a major limitation on the applicability of conventional reducing gas, such as Ar-5% H_2. The reduction was performed by bubbling an Ar-5 % H_2 gas flow through a solution of 98 % hydrazine monohydrate, transferring hydrazine vapour in the furnace. The reduction was performed between 220 and 265 °C for 10 h.

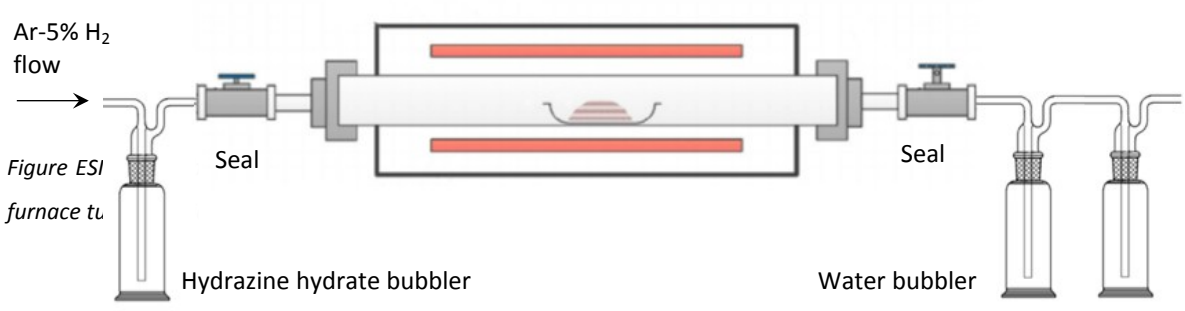

*Figure ESI
furnace tu*

Bulk Bi_2O_3 and $BiCl_3$ powder were used to investigate the influence of different atmospheres on their reduction to metallic Bi. ZnO was used as internal standard to perform Rietveld refinement and calculate the fraction of crystalline vs amorphous Bi, as well as the amount of secondary phases. The heat treatments were conducted in a tubular furnace in a flow of Ar – 5% H_2 gas, either pure or bubbled through a solution of hydrazine monohydrate ($N_2H_4.H_2O$). A flow rate of 20 mL/min was used and the samples were reduced for 10 h at 220 °C, 250 °C, and 265 °C. Hydrazine was used here as it is a powerful and clean reducing agent, since all decomposition products are gaseous.[6,7] However, a minimum concentration of 64 % hydrazine solution is required to obtain sufficient reducing power. Namely, the reducing capacity reduces quickly as the solution becomes more diluted. X-ray diffraction (XRD) patterns of $BiCl_3$ reduced at different temperatures in a flow of Ar - 5% H_2 and in the presence of N_2H_4 vapour are depicted in Figure ESI 8.

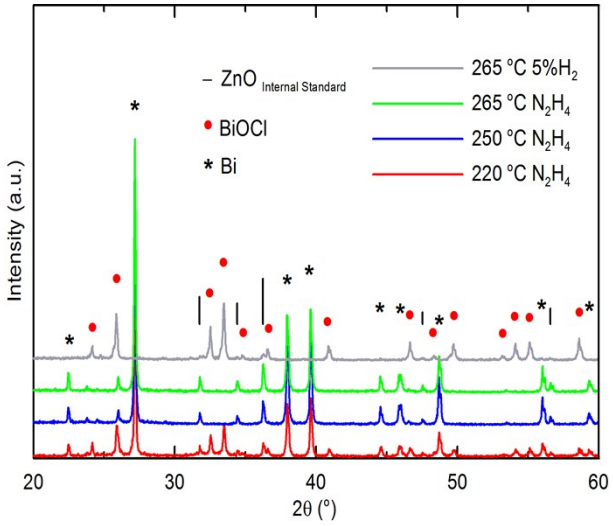

Figure ESI 8. X-ray diffraction patterns of $BiCl_3$ reduced at different temperatures in Ar - 5% H_2 and in the presence of N_2H_4 vapour. The diffraction peaks of the internal standard ZnO, which was used to quantify the amount of crystalline Bi and secondary phase BiOCl.

The Rietveld refining data calculated from the recorded X-ray diffraction pattern is reported in Table ESI 3. It is shows that a minimum temperature of 250 °C and a reduction time of 10 h is required to reduce $BiCl_3$ in N_2H_4 vapour to metallic Bi. In the absence of hydrazine vapour, very little Bi phase was formed when reduced at 265 °C in Ar-5% H_2.

Table ESI 3. Rietveld refinement data of $BiCl_3$ powder reduced at different temperatures and atmospheres for 10 h. The data shows that the presence of N_2H_4 vapour was crucial to reduce $BiCl_3$ to metallic Bi. A temperature of 250 °C and a reduction time of 10 h in N_2H_4 loaded Ar - 5% H_2 was required to reduce $BiCl_3$.

Material	Red. Temp.	Atmosphere	Bi	Bi_2O_3	BiOCl	Amorphous
$BiCl_3$	220 °C	5 % H_2 + N_2H_4	32 %	0 %	17 %	51 %
$BiCl_3$	250 °C	5 % H_2 + N_2H_4	34 %	0 %	0 %	66 %

$BiCl_3$	265 °C	5 % H_2 + N_2H_4	26 %	0 %	0 %	74 %
$BiCl_3$	265 °C	5 % H_2	1 %	0 %	44 %	55 %

Although a minimum temperature of 250 °C was required to reduce bulk $BiCl_3$ powder with N_2H_4, the nanocomposite powders were typically reduced at 220 °C. We believe that the highly exposed surface area facilitated the reduction of $BiCl_3$ – silica nanocomposite powder. Also, we can see from TEM analysis that bismuth leached out of the pore channels upon increasing reduction temperature to 265 °C, as shown in Figure ESI 9. The occurrence of bismuth outside the template can be either by leaching of $BiCl_3$ precursor due to the formation of a melt at 228 °C, or due to the melting of Bi.

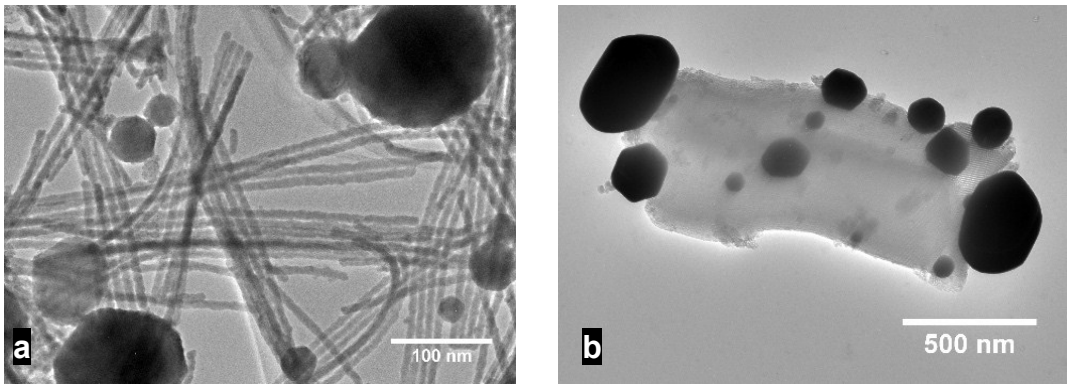

Figure ESI 9. (a) TEM image of 30 v% Bi loaded in SBA-15 and subsequent leaching of the template. $BiCl_3$ was impregnated dissolved in a 20 v% 7.5 mol/L HCl - MeOH solution, with n-octane as non-polar solvent and subsequently reduced at 220 °C in a hydrazine-loaded Ar-5% H_2 gas flow for 10 h. The template was chemically etched with a 1 mol/L NaOH – 0.5 mol/L hydrazine solution for 3 h. (b) TEM image of 30 v% Bi loaded in SBA-15. $BiCl_3$ was impregnated dissolved in a 10 % 7.5 mol/L HCl - MeOH solution, with n-octane as non-polar solvent and subsequently reduced at 265 °C in a hydrazine-loaded Ar - 5% H_2 gas flow for 10 h. The light grey area is the silica template, while the black spheres are bismuth spheres which were formed due to leaching of Bi out of the pores and sintering on the template's exterior surface. Note that the Bi nanowires were compromised during TEM sample preparation, depicting oxidized Bi nanowires.

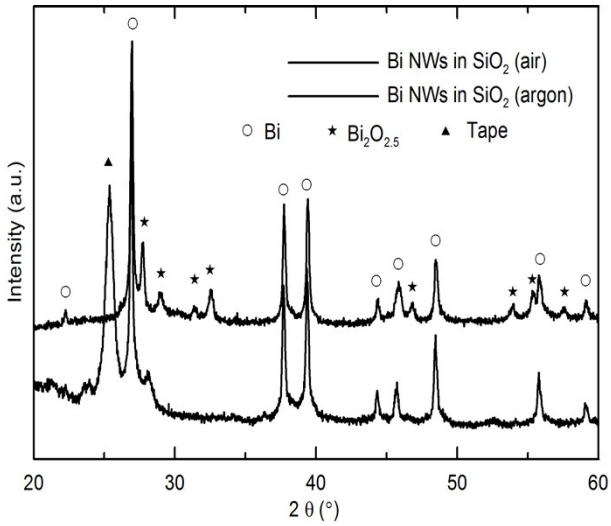

Figure ESI 10. X-ray powder diffraction (XRPD) data of Bi nanowires embedded in KIT-6 mesoporous silica template. (top) Measurement performed under argon atmosphere by applying tape on sample prepared in glovebox. (bottom) XRPD pattern

of same sample without tape shows presence of $Bi_2O_{2.5}$ reflections. The sharp reflections indicate single-crystal nanowires. However, this has not yet been confirmed by HR TEM, as oxidation occurs during TEM sample preparation

After completing the nanocasting process, the replica was separated from the silica template by etching the silica using a 1 mol/L sodium hydroxide solution for 3 h. The nanostructures were recovered through centrifugal separation and washed 4 times with water and ethanol. The N_2 sorption isotherms of mesoporous Bi replicated from a KIT-6 mesoporous silica is shown in Figure ESI 11. The samples were prepared by impregnating a $BiCl_3$ precursor solution in refluxing n-octane or the impregnation of $Bi(NO_3)_3$ in toluene. The composite powders were reduced at 230 °C for 12 h in hydrazine vapour and subsequently the silica template was removed by chemical etching. The powders were dried for 24 h at 140 °C prior to analysis. A BET surface area of 20 and 13 cm^3/g were obtained for the samples prepared with respectively $Bi(NO_3)_3$ and $BiCl_3$. No long-range ordering of the pores was observed in low-angle XRD.

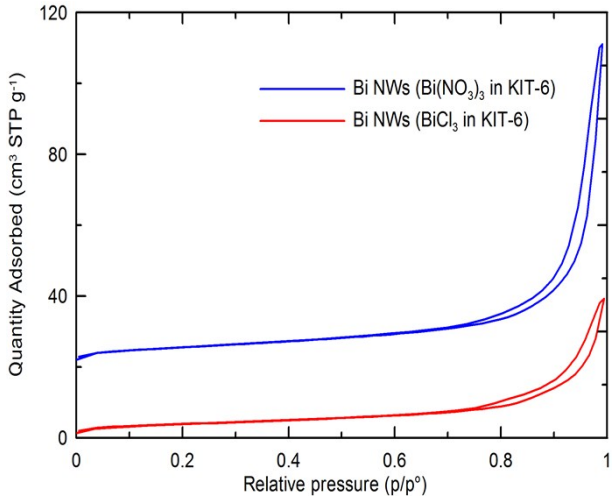

Figure ESI 11. N_2 sorption isotherms of mesoporous Bi replicated from KIT-6 mesoporous silica, by the impregnation of $Bi(NO_3)_3$ or $BiCl_3$ precursor salt, reduction at 230 °C and template removal in 1 mol/L NaOH solution.

6 Synthesis and characterization of Bi – SiO_2 nano composite powder

KIT-6 mesoporous silica was used as template for the synthesis of Bi nanowire composites. The replicated structure after chemically etching the silica template is shown in Figure ESI 12.

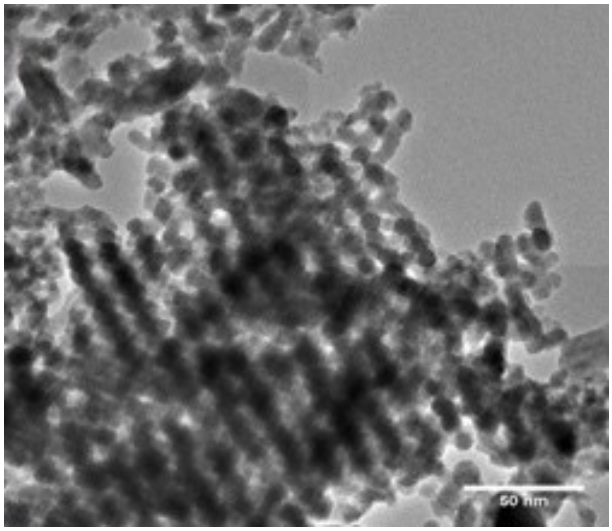

Figure ESI 12. TEM images of Bi nanowire arrays replicated from KIT-6 mesoporous silica. The silica template was impregnated with a $BiCl_3$ precursor in 10 w% HCl – 80 v% MeOH solution, reduced at 220 °C in N_2H_4 vapour for 12 h and subsequently subjected to 1 mol/L NaOH etching solution to remove the silica template. Note that the interconnected Bi nanowires were compromised during TEM sample preparation, depicting oxidized Bi nanowires.

The nanowire composite powder was sintered at 230 °C for 20 min in a vacuum under a uniaxial pressure of 50 MPa and subsequently cut for further analysis. Note that all steps of the sample preparation and electrical measurements were performed in an inert atmosphere.

The effect of the sintering process on the mesoporous silica template was studied by comparing the pore volume of as-synthesized KIT-6 template and template compressed at 230 °C for 20 min at a pressure of 50 MPa, the same conditions subjected to the KIT-6-Bi nanocomposite. The pore volume of the obtained mesoporous silica pellet was reduced by 23% compared to the original powderous KIT-6 sample. Considering the small fraction of Bi inside the template's pores (29 v%), the reduction in pore volume was not considered detrimental for the synthesis of nanocomposite samples.

Further, TEM analysis of KIT-6-Bi nanocomposites after SPS sintering was performed to confirm the presence of Bi nanostructures in the pelletized sample (Figures ESI 13). The TEM sample was prepared by grinding a sintered KIT-6-Bi pellet in a mortar and dispersing the powder in isopropanol by sonication for 1h. The sample was analysed on a Lacey/Carbon 200 Cu grid.

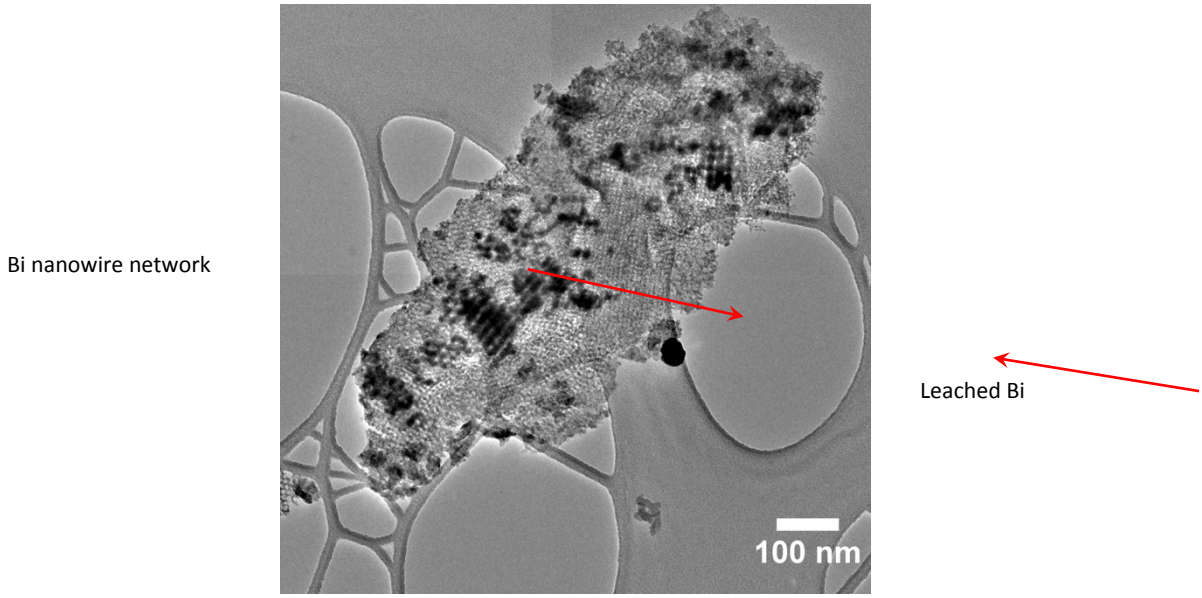

Figure ESI 13. Typical TEM images of the nanocomposite powder after SPS sintering. Bi nanowires are confined within the template's pores, with the presence of a leached Bi sphere at the template's surface as indicated on the figure.

It can be seen from the TEM image in Figure ESI 13 that the Bi nanostructures remained predominantly embedded within the silica template during the sintering process. Consequently, the presence of Bi nanostructures within the nanocomposite sample was confirmed via both TEM analysis and electrical resistivity measurements.

7 References

1. *A. Coelho, Topas Academic v4.1, Coelho Software, Brisbane, Australia, 2007.*

2. Zhao, D.Y., et al., *Nonionic triblock and star diblock copolymer and oligomeric surfactant syntheses of highly ordered, hydrothermally stable, mesoporous silica structures.* Journal of the American Chemical Society, 1998. **120**(24): p. 6024-6036.

3. Kim, T.W., et al., *MCM-48-like large mesoporous silicas with tailored pore structure: Facile synthesis domain in a ternary triblock copolymer-butanol-water system.* Journal of the American Chemical Society, 2005. **127**(20): p. 7601-7610.

4. Huang, X., et al., *Synthesis of confined Ag nanowires within mesoporous silica via double solvent technique and their catalytic properties.* Journal of Colloid and Interface Science, 2011. **359**(1): p. 40-46.

5. Wang, Z.-J., Y. Xie, and C.-J. Liu, *Synthesis and Characterization of Noble Metal (Pd, Pt, Au, Ag) Nanostructured Materials Confined in the Channels of Mesoporous SBA-15.* Journal of Physical Chemistry C, 2008. **112**(50): p. 19818-19824.

6. Littrell, D.M., D.H. Bowers, and B.J. Tatarchuk, *Hydrazine reduction of transition-metal oxides.* Journal of the Chemical Society-Faraday Transactions I, 1987. **83**: p. 3271-3282.

7. Pint, C.L., et al., *Rapid and scalable reduction of dense surface-supported metal-oxide catalyst with hydrazine vapor.* ACS nano, 2009. **3**(7): p. 1897-905.